Visualization of F-actin and G-actin equilibrium using fluorescence resonance energy transfer (FRET) in cultured cells and neurons in slices

Ken-Ichi Okamoto & Yasunori Hayashi

RIKEN-MIT Neuroscience Research Center, The Picower Institute for Learning and Memory, Department of Brain and Cognitive Sciences, Massachusetts Institute of Technology, 46-4243A, 43 Vassar Street, Cambridge, Massachusetts 02139, USA. Correspondence should be addressed to Y.H. (yhayashi@mit.edu).

Published online 3 August 2006; doi:10.1038/nprot.2006.122

The plasticity of excitatory synapses has conventionally been studied from a functional perspective. Recent advances in neuronal imaging techniques have made it possible to study another aspect, the plasticity of the synaptic structure. This takes place at the dendritic spines, where most excitatory synapses are located. Actin is the most abundant cytoskeletal component in dendritic spines, and thus the most plausible site of regulation. The mechanism by which actin is regulated has not been characterized because of the lack of a specific method for detection of the polymerization status of actin in such a small subcellular structure. Here we describe an optical approach that allows us to monitor F-actin and G-actin equilibrium in living cells through the use of two-photon microscopy to observe fluorescence resonance energy transfer (FRET) between actin monomers. Our protocol provides the first direct method for looking at the dynamic equilibrium between F-actin and G-actin in intact cells.

INTRODUCTION

The synapse is a highly specialized structure where various signal transduction molecules and their scaffolding proteins assemble and interact in a hierarchical organization[1]. It is dynamic, rather than static, and is susceptible to bidirectional remodeling according to the intensity of the synaptic input. In hippocampal CA1 pyramidal cells, short bursts of synaptic input induce long-term potentiation (LTP) of synaptic transmission, whereas prolonged low-frequency stimulation induces long-term depression (LTD). Synaptic plasticity has conventionally been studied from the functional aspect using the electrical responses of neurons as the read-out. Recently, a great amount of effort has been made towards elucidation of another aspect of synaptic plasticity, the structural plasticity that is associated with functional change and the molecular mechanisms that are responsible for it[2–6]. These studies have shown that the dendritic spine, which harbors most of the excitatory synapses in these cells, responds quickly to an input stimulus to expand (in the case of LTP) or shrink (LTD) within a few minutes, and these changes are persistent for up to 2 h.

In an effort to elucidate the molecular mechanisms that are associated with structural plasticity, we focused on actin, the primary cytoskeletal component in dendritic spines[7–17]. One of the most intriguing aspects of actin is that it is maintained in equilibrium between two forms, F-actin and G-actin, and that local regulation of this equilibrium is a major target of cellular regulation of motility and structure. Because of the small size of dendritic spines, however, it has remained unclear how this equilibrium between the two forms is regulated by neuronal activity, and there has even been contradiction among reports[12–16]. In view of this, we attempted to monitor this equilibrium optically in the dendritic spines of living neurons.

Experimental design

Background. The distance between actin monomers in F-actin is 55 Å, which is within the typical range for FRET to occur (10–100 Å)[18–21]. Taylor *et al.* used purified and chemically labeled fluorescent actin *in vitro* and observed FRET between actin monomers[18,19]. This FRET is due to intrafilament, rather than interfilament, alignment of donor and acceptor actin, and its efficiency does not depend on filament concentration, thus providing an ideal system for the detection of actin equilibrium in a structure where actin distribution is heterogeneous. We followed this strategy in an updated form using genetically encoded fluorescent actins and showed that we can use FRET to monitor the equilibrium status of actin in living tissue (**Fig. 1**)[2]. This provides information about the equilibrium between F-actin and G-actin. Fluorescently labeled phalloidin stains only F-actin, giving no information about G-actin[13,14]. A GFP fusion protein of actin has been used successfully to depict the cellular distribution and dynamics of actin in

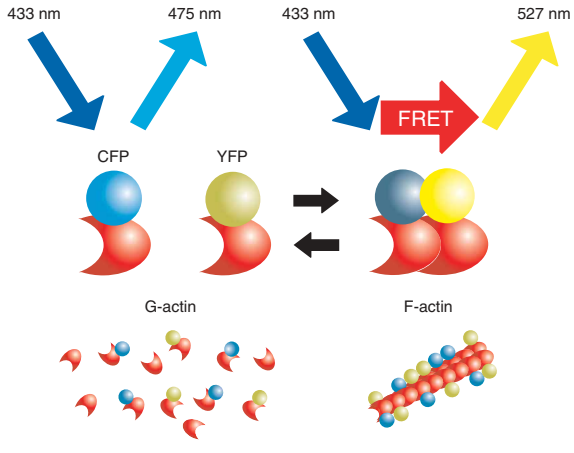

Figure 1 | Strategy of using FRET to detect equilibrium between G-actin and F-actin. The distance between actin monomers in F-actin is 55 Å, which is within the typical range for FRET (10–100 Å). Tagging actin with CFP and YFP as donor and acceptor, respectively, allows us to use FRET to observe the equilibrium between F-actin and G-actin in living cells.

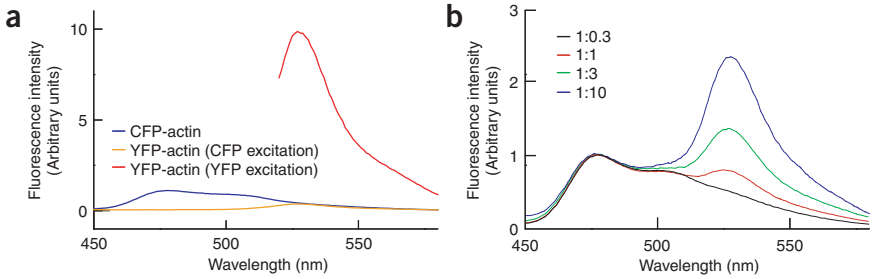

Figure 2 | Emission spectra of HEK293 cell homogenates that express CFP- and YFP-actin individually or together. (**a**) Fluorescence emission spectra of CFP-actin alone at 433-nm excitation (blue line), YFP-actin alone at 433-nm excitation (orange line) and YFP-actin alone at 500-nm excitation (red line). The maximum excitation wavelength for CFP is 433 nm, and 500 nm is approximately half-maximum for YFP. At 433-nm excitation, the fluorescence intensity of YFP-actin is 1–2% of the intensity at the maximum excitation of 514 nm. (**b**) Fluorescence emission spectra of cells that coexpress CFP- and YFP-actin at different ratios. The HEK293 cell homogenate was excited at 433 nm. The spectra are normalized to the CFP (donor) peak. The ratios of CFP-actin and YFP-actin DNAs that were used for the transfection are shown. The CFP peak is at 475 nm, and the YFP peak is at 527 nm.

living tissue, but this cannot distinguish between the two forms of actin[15,17]. In this way, the information obtained with our protocol is unique.

Fluorospectrometric assay. To determine whether cyan fluorescent protein (CFP)-actin and yellow fluorescent protein (YFP)-actin show FRET, we carried out a fluorospectrometric assay using homogenates of HEK293 cells that express CFP-actin or YFP-actin or that express both forms (see PROCEDURE and **Fig. 2**). The spectral profile and its sensitivity to an actin-depolymerizing reagent (data not shown) confirmed that the observed FRET was able to detect F-actin that had formed between CFP-actin and YFP-actin.

Selection of preparation and gene transfection method for imaging. To observe actin filaments in cultured cells, we chose NIH3T3 cells. NIH3T3 cells are of fibroblast origin and have distinct stress fibers, which allow easy observation of actin filaments (see PROCEDURE). Transfection can easily be carried out using a cationic lipid.

To image the modulation of actin under synaptic plasticity in neurons, we decided to use the organotypic slice culture of rat hippocampal slices (see PROCEDURE) for the several advantages it confers[22,23]. Acute slices that are typically used for plasticity studies are not suitable, as we need to incubate the slice for 4–7 d after transfection to let the cells express CFP- and YFP-actin. In slice cultures, as compared with dissociated cultures, the tissue architecture is better preserved; it is easy to identify the cell type being imaged based on location and, furthermore, it is relatively easier to induce synaptic plasticity. The downside is that gene introduction is not as easy as in dissociated culture. This is particularly relevant because we need to express two proteins, CFP-actin and YFP-actin. Here we describe a method that uses a gene-gun for cotransfection[2,24,25]. Typically, the transfection efficiency is one positive CA1 pyramidal neuron per slice. To increase the number of expressing cells, a virus vector may be used. In this case, one needs to use two promoters to express CFP-actin and YFP-actin. Alternatively, one can connect the two open reading frames with an internal ribosomal entry site (IRES)[26]. We obtain the slices from rats, but one should be able to use other species, such as mouse, with minimum modification. Cortical and cerebellar slice cultures have been reported and are readily transfected with the gene-gun as well[24,25].

Selection of microscope. FRET signals can be visualized with a standard fluorescence microscope equipped with appropriate filter sets and a camera, such as a cooled charge-coupled device camera[21,27]. The filter sets (**Table 1**) ideally should be mounted on a motorized filter-wheel to allow quick and vibration-free switches between channels. If a conventional confocal microscope is to be used, the excitation light source must be chosen carefully. The standard Ar laser with which most commercially available confocal microscopes are equipped emits at 457 or 488 nm. These wavelengths excite YFP directly, adding substantial background to the FRET. A shorter wavelength, such as the 442-nm spectral line from a helium-cadmium laser, should be used. Such a laser excites CFP with minimum excitation of the YFP fluorophore. The emission filter should be chosen from **Table 1**.

If the final goal is to visualize FRET between actin that is present deep in tissues, such as in dendritic spines in a slice, the use of a two-photon microscope is recommended. We use a custom-made two-photon microscope based on a *Fluoview FV300* (*Olympus*), with a *Millennia Pro pump laser* (*Spectra-Physics*) and a *Tsunami Ti:Sapphire laser* (*Spectra-Physics*). The Ti:Sapphire laser is tunable,

TABLE 1 | Excitation wavelength and emission filters used for FRET imaging[a].

	Excitation	Emission filter	Dichroic mirror
CFP/YFP FRET (epifluorescent microscope)	440/20 nm[b]	Donor (CFP) channel: 480/30 nm Acceptor (YFP) channel: 535/26 nm	505 nm long-pass
CFP/YFP FRET (two-photon microscope)	800 nm	Donor (CFP) channel: 480/30 nm Acceptor (YFP) channel: 535/26 nm	505 nm long-pass
Texas-Red (epifluorescent microscope)	560/40 nm	635/55 nm	590 nm long-pass
Texas-Red (two-photon microscope)	900 nm	600/100 nm	565 nm long-pass

[a]The optical components for detecting FRET between CFP and YFP are described here for both two-photon microscopy and epifluorescence microscopy. For two-photon microscopy, the emission filters are elements 15 and 16 and the dichroic mirror is element 14 as shown in **Figure 3**.
[b]Bandpass filters are described as center wavelength/bandwidth. For example, 440/20 nm indicates a bandpass filter with a 440-nm center wavelength and 20-nm bandwidth.

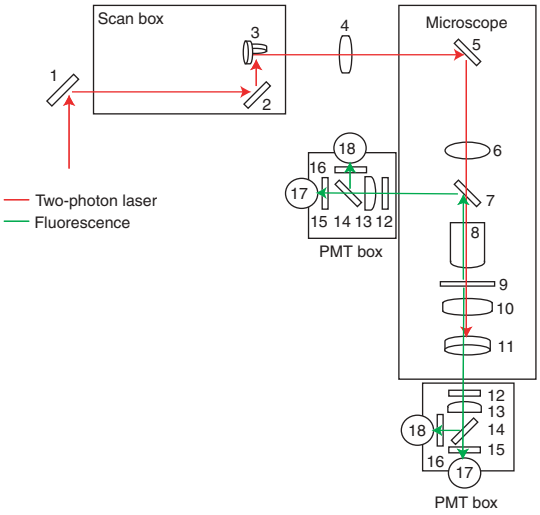

Figure 3 | Configuration of a two-photon laser scanning microscope. The top PMTs (17 and 18) are mounted at the sides of the epifluorescence filter turret, and the bottom PMTs are mounted under the microscope. The signals from the two sets of PMTs are merged electrically and are brought into the computer interface. Other elements are as follows: 1 and 2, mirrors; 3, galvano mirror; 4, transfer lens; 5, mirror; 6, tube lens; 7, dichroic mirror (700 nm long-pass); 8, objective lens (LUMPL60XW/IR-2, Olympus); 9, sample; 10, condenser lens (n.a., 1.4; oil); 11, dichroic mirror (700 nm short-pass); 12, laser blocking filter (700 nm short-pass); 13, lens; 14, dichroic mirror; 15, YFP emission filter; 16, CFP emission filter; 17, PMT for YFP channel; 18, PMT for CFP channel. See **Table 1** for more information on elements 14–16. Optics necessary for conventional fluorescence excitation and detector are not described.

and it is relatively easy to select a donor-specific excitation wavelength. We tested several different excitation wavelengths and chose 800 nm. At a shorter wavelength (<780 nm), excitation light leaks through the YFP emission filter and increases the background noise. Also, YFP has a minor excitation peak at around 400 nm (at one-photon excitation) that seems to be excited at <780 nm under two-photon microscopy and also increases the YFP channel background noise. Shorter wavelengths also contribute to a markedly higher autofluorescence of tissue, which impedes deep imaging in tissue slices. At longer wavelengths (>820 nm), direct excitation of YFP interferes with imaging. Furthermore, the Ti:Sapphire laser has maximum power and stability at around 780–800 nm. Other optical components and settings for imaging are shown in **Table 1** and **Figure 3**. Place photomultiplier tubes (PMTs) as close to the sample as the situation allows. Installing a second set of PMTs underneath the microscope to detect the transfluorescence signal from the sample through the condenser lens approximately doubles the signal intensity, although this requires engineering of both the microscope and electrical circuit and is not an absolute requirement.

It is advisable to image control cells that express only CFP-actin or YFP-actin to characterize optical properties of the system used for the detection. CFP and FRET (YFP) images are much dimmer than images of GFP-actin, because narrow band-pass filters are used for taking images. The CFP signal inevitably leaks into the YFP channel, which should always be taken into consideration. Because the magnitude of the leak is constant irrespective of FRET status, it should not largely affect the results. In our system, the leak of CFP fluorescence into the YFP channel represents 31% of the reading of the CFP channel. YFP is minimally excited at 800 nm.

Phalloidin staining. To confirm that the visualized structures are F-actin filaments in cultured cell lines, staining with Texas red–phalloidin is useful. This staining has to be done in fixed cells and gives a stronger signal than fluorescent protein imaging. Once stained, the cells are no longer suitable for FRET imaging. Ideally, the same cell should be identified in both FRET imaging and phalloidin staining. Coverslips with a photoetched grid (for example Photoetched Cover Slips, Bellco, cat. no. 1916-91818) may be helpful.

Image analysis. To visualize the FRET data, the intensity-modulated display (IMD) mode with which Metamorph is equipped is often used. In this mode, hue indicates the YFP/CFP ratio, whereas brightness indicates the intensity of the CFP channel. Incorporating the latter factor avoids showing a noisy and uninformative ratio in areas where fluorescence intensity is close to the background amount. IMD is suitable only for visualization purposes. Quantitative analyses have to be done by using readings from the region of interest (ROI) drawn on individual spines. Metamorph has various functions for this purpose. Spines that are well separated from the dendritic shaft or from other spines should be selected for analysis. To carry out quantitative analysis on noncommercial software, ImageJ by W. Rasband (http://rsb.info.nih.gov/ij/) with UCSD Confocal Microscopy Plugins by P. Kelly and H.J. Karten (http://rsb.info.nih.gov/ij/plugins/ucsd.html) is useful. This program does not, however, support the IMD mode of visualization.

From Metamorph version 6.0 on, there is a FRET menu. We do not use this function because it requires an acceptor image at acceptor-specific excitation in addition to donor and acceptor (FRET) images at donor-specific excitation. Although this is ideal for calculating FRET efficiency, in two-photon microscopy it is not practical to switch the excitation wavelength back and forth between 800 nm and the YFP-specific wavelength, which is >900 nm, during a rapid time-lapse imaging experiment unless one is equipped with two Ti:Sapphire lasers. If one uses a standard fluorescence microscope, it is rather easy to change the excitation wavelength to take acceptor-specific imaging, and this functionality of Metamorph becomes useful.

Choice of fluorophore. The combination of CFP and YFP for FRET donor and acceptor is currently the best combination available, but it is still not optimal because of the low overall signal and the leak of donor (CFP) fluorescence to the acceptor (YFP) channel. We have tried other fluorescent proteins, such as monomeric derivatives of DsRed[28,29], in combination with GFP-actin as the donor, but there was little improvement. Tandem dimeric derivatives of DsRed[28,29], such as tdimer, are reported to be brighter but are twice the size of GFP. This is likely to affect the diffusion kinetics of the fusion protein. Actin in the dendritic spine turns over very rapidly with the pool of actin in the dendritic shaft[17]. Therefore, the attachment of donor and acceptor with two fluorescent proteins of different size may complicate the results, because the smaller molecule moves faster than the larger molecule, which results in a false-positive change in the donor/acceptor ratio.

This is a unique issue of FRET between actin monomers and is not applicable to most other FRET probes.

Limitations of the method. This method does have certain limitations. The FRET value represents the equilibrium between F-actin and G-actin, but it does not represent the total amount of F-actin itself. These are related but independent parameters. The FRET value also does not give the absolute ratio of F-actin to G-actin, because FRET efficiency depends on the relative amounts of donor actin, acceptor actin and endogenous unlabeled actin (**Fig. 2b**). The inclusion of unlabeled actin in a filament decreases the chance for donor actin and acceptor actin to be aligned within the effective distance. In contrast, an excess of acceptor actin as compared with donor actin increases the chance that the acceptor will be located next to the donor, thereby increasing the FRET whereas the overall signal intensity decreases. Because of this, we do not recommend comparing FRET efficiencies across different neurons. The best application of this method will be time-lapse imaging or comparison across different structures within the same cell. It should also be noted that FRET potentially detects cross-bundling of F-actin filaments in the presence of bundling protein.

Application of other FRET probes in synaptic imaging. Imaging methods that are described here can be used for various FRET constructs that have been reported to date[27] to elucidate biochemical processes taking place locally at the synapse. Compared with larger structures, in which most of these FRET probes have been characterized and used, the synapse is significantly smaller, and the effect of diffusion of the optical probes becomes more substantial. A change in the FRET signal may indicate either the spread of the biochemical signal, the event that the probe is detecting or the diffusion of the probe itself. A FRAP (fluorescence recovery after photobleaching) assay is an easy test to estimate the diffusion rate of the FRET probe[21]. If it is significantly faster than the molecules or the event that the probe is designed to detect, the kinetics and distribution of the FRET signal do not necessarily represent the localization or the time course of the target molecule or event. In the worst scenario, the diffusion of the probe dilutes out the change and can give a false negative. Inserting a synapse tagging signal such as the PDZ domain protein–binding ligand may prevent the diffusion of the FRET probe[30].

In the case of actin, this raises an interesting issue. The actin molecule itself is constantly being replaced at the synapse[17], but the different amounts of G-actin and F-actin equilibrium are maintained at the level of the individual synapse[2]. The mechanism for this is currently under investigation.

FRET probes are often designed based on functional domains of various proteins. For actin, so far we and others have not seen any particular impairment of synaptic structure and function by overexpression of actin tagged with fluorescent proteins[2,17]. Any FRET probe should be carefully characterized to confirm that its expression does not have an effect on synaptic structure and function.

Additional information. Readers may refer to review articles for more general information about fluorescent proteins, FRET and two-photon microscopy[21,27,31–34].

MATERIALS

REAGENTS

- Mammalian expression vectors for CFP-actin and YFP-actin
- HEK293 cells, NIH3T3 cells or postnatal day (P) 6–7 rat hippocampal organotypic slice cultures prepared as described[2,22,23]
- Lipofectamine 2000 (Invitrogen; for HEK293 cells only)
- F-actin assay buffer: 10 mM PIPES, 1 mM $MgCl_2$, 1 mM ATP and 0.5 mM DTT (pH 7.0; store at –20 °C; for HEK293 cells only)
- Latrunculin A (Molecular Probes; optional): 10 mM stock in DMSO
  ! CAUTION Toxic.
- Jasplakinolide (Molecular Probes; optional; for NIH3T3 cells only)
- Lipofectin with Plus Reagent (Invitrogen; for NIH3T3 cells only)
- Paraformaldehyde (for NIH3T3 cells only) **! CAUTION** Toxic.
- Triton X-100 (for NIH3T3 cells only)
- Texas red–phalloidin (Molecular Probes; for NIH3T3 cells only)
  ! CAUTION Toxic.
- FluoSpheres polystyrene microspheres, 1.0 μm (Molecular Probes, cat. no. F-13081; optional; for hippocampal organotypic slice cultures only)
- Glass capillaries (for example, Harvard Apparatus, cat. no. GC200F-10; optional, for hippocampal organotypic slice cultures only)
- Basal-buffered saline (BBS): 135 mM NaCl, 5.4 mM KCl, 11 mM glucose, 2.5 mM $CaCl_2$, 1 mM $MgCl_2$, 20 mM HEPES-Na (pH 7.4; for NIH3T3 cells only)
- Artificial cerebrospinal fluid (ACSF; see REAGENT SETUP; for hippocampal organotypic slice cultures only)
- Reagents for HEK293 cell culture, NIH3T3 cell culture or organotypic culture of hippocampal slices[23]
- Reagents for making gene-gun bullets including 1.6-μm gold particles (Bio-Rad and others)

EQUIPMENT

- 35-mm tissue culture dishes or 6-well tissue culture plates (for HEK293 cells only)
- 24-well tissue culture plates and 8 × 8–mm glass coverslips (for NIH3T3 cells only)
- Millicell-CM membranes (Millipore, cat. no. PICM0RG50; for hippocampal organotypic slice cultures only)
- Glass-Teflon homogenizer (for HEK293 cells only)
- Fluorospectrometer (for HEK293 cells only)
- Helios Gene-Gun (Bio-Rad; for hippocampal organotypic slice cultures only)
- Two-photon laser scanning microscope (we used a custom-made system based on the Fluoview FV-300 (Olympus) with a Millennia Pro pump laser (Spectra-Physics) and a Tsunami Ti:Sapphire laser (Spectra-Physics); for NIH3T3 cells and hippocampal organotypic slice cultures only)
  ! CAUTION Practice necessary precautions and wear eye protection when working with a laser.
- Imaging chamber (custom made from Plexiglas with a coverglass on the bottom; for NIN3T3 cells and hippocampal organotypic slice cultures only)
- Peristaltic pump (for example, Rainin, model no. RP-1; for hippocampal organotypic slice cultures only)
- Slice holder: custom made from U-shaped platinum wire (~1 cm × 1 cm; original diameter of wire is 1 mm but flattened with a hammer to ~300 μm) and fiber separated from nylon stockings
- Dissecting microscope (for hippocampal organotypic slice cultures only)
- Manipulator (for example, Sutter Instruments, model no. MP-285; for hippocampal organotypic slice cultures only)
- Stimulator (for example, Master 8, A.M.P.I.; for hippocampal organotypic slice cultures only)
- Isolator (for example, ISO-Flex, A.M.P.I.; for hippocampal organotypic slice cultures only)
- Metamorph (Molecular Devices; for NIH3T3 cells and hippocampal organotypic slice cultures only)
- Glass puller (for example, Sutter Instruments, model P-97; optional, for hippocampal organotypic slice cultures only)

REAGENT SETUP

ACSF Prepare a solution containing 119 mM NaCl, 2.5 mM KCl, 4 mM $MgCl_2$, 26.2 mM $NaHCO_3$, 1 mM NaH_2PO_4 and 11 mM glucose. Store up to 1 month at 4 °C. Bubble and equilibrate the solution with 5% CO_2/95% O_2 just before use and then add 4 mM $CaCl_2$.

PROCEDURE

1| Prepare mammalian expression vectors containing CFP-actin and YFP-actin and purify plasmid DNA for each construct. We obtained these constructs by replacing EGFP of EGFP–human β-actin (Clontech) with ECFP (Clontech) and an improved version of YFP (a Venus variant; ref. 35) with increased brightness and lowered pH sensitivity. These constructs are available on request. The original YFP is sensitive to a change in pH around 7 and is therefore not suitable for *in vivo* imaging.

● **TIMING** Subcloning will require about 1 week. Once the constructs are made (or if the clones are obtained from somewhere), about half a day is needed to purify plasmid DNA.

2| Prepare an appropriate culture for fluorospectrometric assays in HEK293 cells (A), for imaging of non-neuronal (NIH3T3) cells on coverslips (B) or for imaging of neuronal cells from hippocampal organotypic slice cultures (C).

● **TIMING** Culture preparation requires approximately 1 h.

(A) To prepare HEK293 cells for fluorospectrometric assays

(i) Plate cells at 5×10^5 cells per 35-mm dish (or per well of a 6-well plate) and incubate overnight in a 37 °C incubator with 5% CO_2.

(B) To prepare for imaging of non-neuronal (NIH3T3) cells on coverslips

(i) Plate NIH3T3 cells at 3×10^4 cells per well in a 24-well plate containing one 8 × 8–mm glass coverslip per well and incubate overnight in a 37 °C incubator with 5% CO_2.

(C) To prepare for imaging of neuronal cells from hippocampal organotypic slice cultures

(i) Place P6–7 rat hippocampal organotypic slice cultures on Millicell-CM membranes as described[22,23]. We use a low-profile membrane. One membrane can carry three or four slices. Place the slices close to the center of the membrane so that they are more efficiently transfected by the gene-gun. Culture slices for 4–5 d *in vitro* (DIV4–5) in a 35 °C incubator with 5% CO_2 while changing medium[23] approximately every 2 d.

▲ **CRITICAL STEP** Transfection efficiency (Step 3C) is best between DIV4 and 7. Before DIV4, slices are covered with cell debris from the slicing process, making them difficult to transfect. After DIV7, transfection efficiency decreases, possibly because of glial proliferation.

3| Transfect DNA in HEK cells (A), in NIH3T3 cells (B) or in neurons of hippocampal slices with a gene-gun (C).

● **TIMING** Transfecting DNA for cell cultures requires about 1 h. To prepare gene-gun bullets for the hippocampal slices requires 1 h, at which point transfection (i.e., shooting) takes about 5 min.

(A) Transfect DNA in HEK293 cells

(i) Transfect CFP- and YFP-actin expression vectors at a ratio of 1:3 (total 2 μg DNA per 35-mm dish) using Lipofectamine 2000 according to the manufacturer's protocol. Other methods of transfection may be used as well.

(B) Transfect DNA in NIH3T3 cells

(i) Transfect CFP- and YFP-actin expression vectors at a ratio of 1:3 (total 1 μg DNA per well) using Lipofectin with Plus Reagent according to the manufacturer's protocol. Other methods of transfection may be used as well.

(C) Transfect DNA in neurons in hippocampal slices with a gene-gun

(i) Prepare bullets for gene-gun that carry CFP-actin and YFP-actin expression vectors at a ratio of 1:3 using a total of 100 μg DNA for 12.5 mg of 1.6-μm gold particles according to the manufacturer's protocol. Store at –20 °C for up to 1–2 months under desiccation.

(ii) Shoot the slices with bullets at 160 psi using a Helios Gene-Gun.

4| Proceed with fluorospectrometry for HEK293 cell homogenate (A) or with two-photon microscopy for NIH3T3 cells (B) or for neurons from hippocampal organotypic slice cultures (C).

● **TIMING** Processing either the HEK293 or NIH3T3 cells requires about 1–2 h; about 3 h is required to process the neurons in each slice.

(A) Fluorospectrometry for HEK293 cell homogenate

(i) After 2–3 d in culture, wash the cells once in 1–2 ml PBS and then resuspend in 1 ml PBS by gently applying flow using a Pasteur pipette. Transfer cells into a 1.5-ml microcentrifuge tube and centrifuge at 3,000*g* for 1 min at room temperature (20–25 °C). Resuspend the cell pellet in 0.5 ml F-actin assay buffer and homogenize cells using a glass-Teflon homogenizer.

(ii) Centrifuge cells at 3,000*g* for 1 min at room temperature to clear large cell debris.

? TROUBLESHOOTING

(iii) Transfer supernatant to a cuvette and monitor fluorescence emission profile between 450 and 550 nm in the fluorospectrometer at 433-nm excitation (**Fig. 2**).

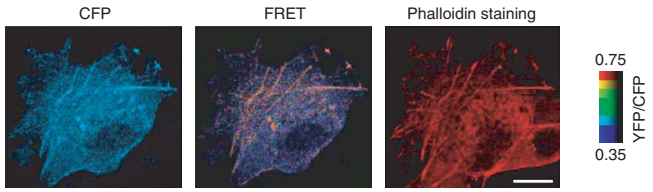

Figure 4 | FRET image of an NIH3T3 cell transfected with CFP- and YFP-actin. The cell was observed under a two-photon laser scanning microscope with CFP-specific excitation at 800 nm. The CFP image (left) represents the distribution of fluorescent actin. The FRET image (middle) is shown in IMD mode. F-actin (right) was stained with Texas red–phalloidin after fixation. There is an untransfected cell on the right. Color scale on the far right. Note the high FRET signal (warmer hue) that is colocalized with actin filaments. Scale bar, 5 μm.

(iv) Optionally, to confirm that the FRET signal is due to polymerized actin, add latrunculin A (10 μM final concentration) into the cuvette and monitor the fluorescence profile (see ANTICIPATED RESULTS).

(B) Two-photon microscopy for NIH3T3 cells

(i) After 1–2 d in culture, visualize each coverslip in an imaging chamber filled with BBS solution with a two-photon microscope. Image both CFP and YFP channels simultaneously at the CFP-specific excitation (800 nm; **Fig. 4**).

(ii) Optionally, to confirm FRET, carry out acceptor bleaching. Photobleach YFP specifically at 525/45 nm (525-nm center wavelength and 45-nm band width) for 1 min with light from the mercury lamp. Take another FRET image (see ANTICIPATED RESULTS).

(iii) Optionally, to stain NIH3T3 cells with fluorescent phalloidin, fix cells with 4% (wt/vol) paraformaldehyde in PBS for 30 min on ice, wash with PBS twice and permeabilize them with 0.5% (vol/vol) Triton X-100 in PBS for 5 min. Wash again with PBS. Stain cells with Texas red–phalloidin (1:100 dilution of the stock solution supplied by Molecular Probes in PBS) for 1 min. Wash again in PBS. Visualize stained stress fibers under two-photon microscopy according to the optical settings in **Table 1**. The fibrous structure will be stained with Texas red–phalloidin.

? TROUBLESHOOTING

(C) Two-photon microscopy for neurons from hippocampal organotypic slice cultures

(i) Cut out the membrane with a slice on it 4–7 d after transfection using a sharp surgical blade under a dissecting microscope.

▲ **CRITICAL STEP** Do not let the slices dry. Once a membrane is being used, it is advisable to keep it in a separate CO_2 incubator. Repeated opening and/or closing of the incubator changes the CO_2 concentration and may affect the condition of the remaining cultures. We typically move one membrane to a 35-mm dish with ~0.9 ml culture medium and keep it in a separate, small CO_2 incubator.

(ii) Transfer the slice to the imaging chamber on the two-photon microscope and continuously perfuse with ACSF using a peristaltic pump. Hold the slice with an appropriate holder.

(iii) Search for transfected cells by visual inspection using conventional fluorescence microscopy under the YFP filter set (**Table 2**). Once cells are found, switch to the CFP filter set and confirm that CFP is expressed. Then switch to two-photon microscopy and zoom into a transfected dendrite in the stratum radiatum. We use a 60× objective lens and 5× digital zoom.

▲ **CRITICAL STEP** A bright cell must be chosen. The ratio of expression of CFP-actin to YFP-actin is also important. When we search for transfected cells, we compare expression using both CFP and YFP filter sets (**Table 2**) and empirically choose cells expressing CFP- and YFP-actin at a 1:3 ratio. To prevent photobleaching, the search time must be minimized as much as possible.

(iv) Take a stack of images. For dendritic spine images, a 0.5-μm *z* interval is used. We typically do not use Kalman averaging to avoid photobleaching. For lower resolution images, larger *z* intervals can be used. If time-lapse imaging is desired, a practical sampling interval is 2–3 min because of photobleaching during imaging. In cells with very high expression, the interval can be reduced to as low as 20 s (**Fig. 5**). Use minimum laser power and increase the PMT sensitivity as much as is practical to avoid photobleaching.

(v) Optionally, to stimulate the neuron, first use a glass puller and a glass capillary to make a glass electrode. One similar to a typical patch electrode (tip resistance ~5 MΩ) may be used for this purpose. Place the glass electrode filled with ACSF 5–15 μm from the dendrite using a manipulator. Apply a train of pulses at <9 V and 100-μs duration at different frequencies and pulse numbers. A Master-8 stimulator in combination with the ISO-Flex isolator allows a flexible programming of

TABLE 2 | Filter sets for epifluorescence detection[a].

	Excitation filter	Dichroic mirror	Emission filter
CFP	440/20 nm[b]	455 nm long-pass	480/30 nm
YFP	495/10 nm	505 nm long-pass	535/26 nm

[a]This is used for visual identification of transfected cells. The filters are housed in a turret wheel and switched with a dichroic mirror (**Fig. 3**, element 7) when fluorescence is visualized with the observer's eyes.
[b]Bandpass filters are described as center wavelength/bandwidth. For example, 440/20 nm indicates a bandpass filter with a 440-nm center wavelength and 20-nm bandwidth.

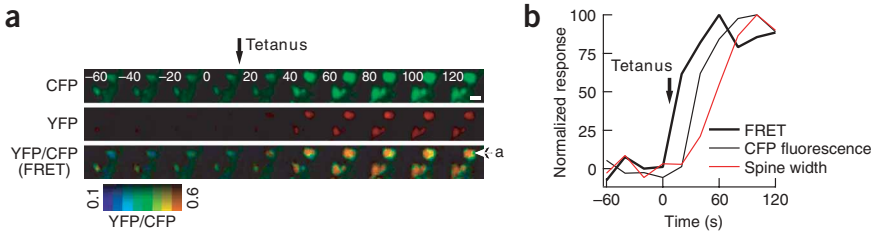

Figure 5 | An example of changes in FRET in response to tetanic stimulation. (**a**) A dendritic segment that expresses CFP- and YFP-actin was tetanically stimulated (100 Hz, 1s). Background-subtracted images in CFP and FRET (YFP) channels and the FRET image in IMD are shown. Time stamp is in seconds. Scale bar, 1 μm. (**b**) Quantitative analysis of the spine that is indicated by the white arrow in **a**. The ratio of CFP and YFP, CFP fluorescence intensity and spine width are plotted versus time. The average of the baseline was taken as 0 and the maximum change was taken as 100. Actin starts polymerizing locally at the dendritic spine, thereby recruiting new actin molecules from the dendritic shaft, most likely by diffusion, although an active mechanism cannot be totally ruled out. This results in the expansion of dendritic spine width. Note that CFP fluorescence is underestimated because of quenching by FRET.

stimulation paradigm. To help with visualization, add fluorescent beads (FluoSphere) to the ACSF used to fill the electrode. The beads attach to the inner wall of the electrode but do not clog the electrode tip. Place the electrode close to the transfected dendrite with visual guidance under two-photon microscopy.

(vi) To confirm FRET, carry out acceptor bleaching of actin as described in Step 4B (ii).

(vii) Optionally, apply latrunculin A or jasplakinolide (both to a final concentration of 10 μM) to confirm that FRET can detect changes in F-actin and G-actin equilibrium.

Analyzing FRET images (NIH3T3 cells and neurons from hippocampal organotypic slice cultures only)

5| Open images in Metamorph and separate them into two channels [menu-display-color separate].

● **TIMING** Each set of images will require 5–60 s, depending on the resolution and the number of stacks.

6| Subtract the background signal from each image [menu-process-use region for background].

● **TIMING** Each set of images will require 5–60 s, depending on the resolution and the number of stacks.

7| Sum the stack images [menu-process-stack arithmetic-operation sum of]. The median filter may be applied at this point [menu-process median filter-source (select image name), dest (new image name), horizontal size, vertical size, sub-sample ratio (find optimal settings)].

● **TIMING** Each set of images will require 5–60 s, depending on the resolution and the number of stacks.

8| Calculate the ratio image for FRET [menu-process-ratio images-numerator (select FRET (YFP) image), denominator (select CFP image), ratio image (select ratio), IMD display (8–16 should be sufficient), IMD intensity (automatically determined by the number of colors chosen in "IMD display")]. Choose [min ratio] and [max ratio] so that the full hue range is utilized.

● **TIMING** This step requires 10 s.

● **TIMING**

Step 1 requires about 1 week for subcloning. Once cloning is done (or if the clones are obtained from somewhere), about half a day is needed to purify the plasmid DNA. Step 2 requires 1 h. Step 3 requires about 1 h for the HEK293 and NIH3T3 cells; 1 h is also needed to prepare the gene-gun bullets for the hippocampal organotypic slice cultures. Once prepared, the shooting (i.e., transfection) of the slices takes approximately 5 min. Step 4 requires 1–2 h for the HEK293 and NIH3T3 cells and about 3 h per slice for the hippocampal cultures. These steps should be repeated as needed; the entire procedure may take weeks depending on the experimental design. Steps 5–8 require about 5 min per image; depending on the goal of the analysis, the data analysis can also take up to a few days.

? TROUBLESHOOTING

HEK293 cell homogenate

Centrifugation removes a portion of F-actin in the pellet. If the YFP peak is not observed or overall fluorescence is very weak, it may be due to the removal of a large amount of F-actin from the supernatant. In such a case, first confirm the expression of YFP-actin by 500-nm excitation and measure emission between 520 nm and 625 nm (**Fig. 2a**). If the YFP-actin peak is observed at 527 nm, increase the extent of homogenization and/or decrease the centrifuge speed. This leaves larger cell clumps in the supernatant, which may cause scattering of the excitation light and result in inaccurate measurements of the CFP peak. To avoid this problem, narrow the slit of the fluorospectrometer as much as is practical. Changing the DNA ratio of CFP- and YFP-actin may also be helpful. A higher ratio of YFP-actin to CFP-actin increases FRET, but the overall signal will become weaker. This becomes important in the imaging studies described below.

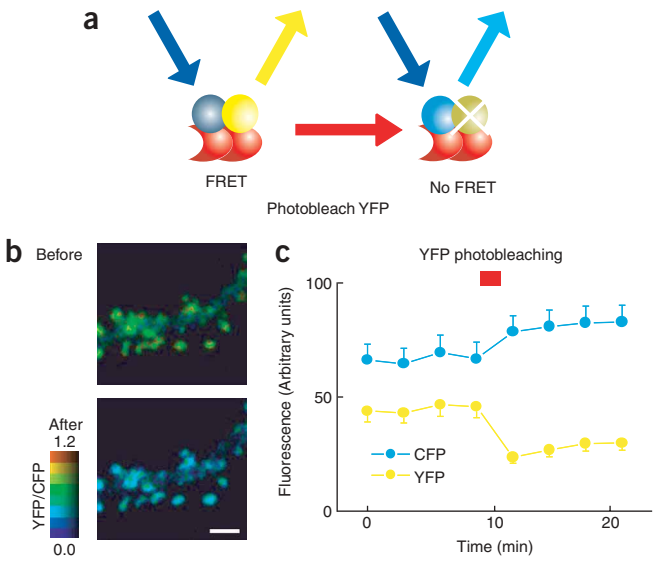

Figure 6 | An example of an acceptor bleaching experiment. (**a**) Schematic illustration of the principle of acceptor bleaching. When the acceptor (YFP) is photobleached, the emission from CFP is dequenched. (**b**) Two-photon microscopic images (shown in IMD) of a dendritic segment of a neuron that expresses CFP-actin and YFP-actin before and after acceptor bleaching. Scale bar, 2 μm. (**c**) Plots of fluorescence intensity in CFP and FRET (YFP) channels in dendritic spine heads. At the indicated point (red square), the acceptor (YFP) was photobleached. Note the increased signal in the CFP channel that was due to dequenching. The remaining signal in the YFP channel is a leak of the CFP signal. Error bars indicate s.e.m.

Texas red–phalloidin staining

If one cannot see stress fibers with Texas red–phalloidin staining, the cell conditions may not be optimal. This may be due to too high a density of cells, poor culture conditions or poor attachment to the coverslips. One can reduce cell density, try a different coverslip or calf serum, or coat the coverslips with collagen or poly-D-lysine.

ANTICIPATED RESULTS

HEK293 cell homogenates

The CFP fluorescence peak is observed at 475 nm with 433-nm excitation. If there is FRET, a second distinct peak representing YFP emission should be observed in cotransfected cells at 527 nm but not in cells expressing CFP-actin only (**Fig. 2a,b**). Furthermore, the pharmacological disruption of actin (e.g., with latrunculin A) will decrease the magnitude of the FRET (YFP) peak, whereas the CFP peak will increase.

Imaging in NIH3T3 cells

By cotransfecting cells with CFP-actin and YFP-actin, FRET can be observed between CFP-actin and YFP-actin that colocalizes with the stress fibers (**Fig. 4**). This experiment is a good control for imaging before moving on to neurons.

Imaging in neurons

Dendritic spine heads have higher FRET than the dendritic shafts do, although it may not be apparent until an off-line analysis is completed. Tetanic stimulation enlarges the dendritic spine head and increases FRET (**Fig. 5**). Prolonged low-frequency stimulation causes an opposite effect. Because axons are stimulated at random, in many cases the stimulated axons do not necessarily form synapse with the dendritic spine under observation and only about 30% of the trials are successful as judged from the spine enlargement after tetanic stimulation. Also, the number of spines that respond varies significantly between experiments. If no effect is observed, tweak the positioning of the electrode. It is advisable to carry out a control experiment using cells loaded with a Ca^{2+} indicator dye such as Oregon-green, if the technique is readily available. A control experiment using a glutamate receptor antagonist may also be necessary to confirm that the phenomenon observed is mediated by synaptically released glutamate. If precise stimulation of a single identified dendritic spine is desired, two-photon uncaging of caged glutamate will be a method of choice[3,36].

Bleaching

An example of acceptor bleaching in neurons is shown (**Fig. 6**). Acceptor photobleaching should eliminate the FRET signal while increasing the CFP signal because of dequenching. FRET efficiency is calculated from the efficiency of dequenching of the CFP signal after specifically photobleaching the acceptor according to the formula

$$\text{Efficiency} = \frac{F_{\text{CFP,after}} - F_{\text{CFP,before}}}{F_{\text{CFP,after}}}$$

$F_{\text{CFP, before}}$ and $F_{\text{CFP, after}}$ represent the CFP signal before and after YFP bleaching, respectively. In our typical neuronal images, the efficiency is 20–30%. The experimental design section (see INTRODUCTION) describes the factors that determine FRET efficiency.

Pharmacological manipulations

Latrunculin A will cause depolymerization of F-actin in dendritic spines, which reduces FRET and eventually causes a loss of dendritic spines. Jasplakinolide causes polymerization and increases FRET.

ACKNOWLEDGMENTS We thank T. Nagai and A. Miyawaki for discussions and sharing resources, S.M. Kwok for sharing spectral data of CFP-actin and YFP-actin and M. Churchill and T. Emery for editing. Supported by RIKEN, The Ellison Medical Foundation and a National Institutes of Health R01 grant (DA017310-01A1) to Y.H.

COMPETING INTERESTS STATEMENT The authors declare that they have no competing financial interests.

Published online at http://www.natureprotocols.com/
Reprints and permissions information is available online at http://npg.nature.com/reprintsandpermissions

1. Sheng, M. & Pak, D.T. Ligand-gated ion channel interactions with cytoskeletal and signaling proteins. *Annu. Rev. Physiol.* **62**, 755–778 (2000).
2. Okamoto, K., Nagai, T., Miyawaki, A. & Hayashi, Y. Rapid and persistent modulation of actin dynamics regulates postsynaptic reorganization underlying bidirectional plasticity. *Nat. Neurosci.* **7**, 1104–1112 (2004).
3. Matsuzaki, M., Honkura, N., Ellis-Davies, G.C. & Kasai, H. Structural basis of long-term potentiation in single dendritic spines. *Nature* **429**, 761–766 (2004).
4. Hayashi, Y. & Majewska, A.K. Dendritic spine geometry: functional implication and regulation. *Neuron* **46**, 529–532 (2005).
5. Zhou, Q., Homma, K.J. & Poo, M.M. Shrinkage of dendritic spines associated with long-term depression of hippocampal synapses. *Neuron* **44**, 749–757 (2004).
6. Nägerl, U.V., Eberhorn, N., Cambridge, S.B. & Bonhoeffer, T. Bidirectional activity-dependent morphological plasticity in hippocampal neurons. *Neuron* **44**, 759–767 (2004).
7. Blomberg, F., Cohen, R.S. & Siekevitz, P. The structure of postsynaptic densities isolated from dog cerebral cortex. II. Characterization and arrangement of some of the major proteins within the structure. *J. Cell Biol.* **74**, 204–225 (1977).
8. Lisman, J. Actin's actions in LTP-induced synapse growth. *Neuron* **38**, 361–362 (2003).
9. Fifková, E. & Morales, M. Actin matrix of dendritic spines, synaptic plasticity, and long-term potentiation. *Int. Rev. Cytol.* **139**, 267–307 (1992).
10. Matus, A. Actin-based plasticity in dendritic spines. *Science* **290**, 754–758 (2000).
11. Colicos, M.A., Collins, B.E., Sailor, M.J. & Goda, Y. Remodeling of synaptic actin induced by photoconductive stimulation. *Cell* **107**, 605–616 (2001).
12. Hering, H. & Sheng, M. Activity-dependent redistribution and essential role of cortactin in dendritic spine morphogenesis. *J. Neurosci.* **23**, 11759–11769 (2003).
13. Fukazawa, Y. *et al.* Hippocampal LTP is accompanied by enhanced F-actin content within the dendritic spine that is essential for late LTP maintenance *in vivo*. *Neuron* **38**, 447–460 (2003).
14. Halpain, S., Hipolito, A. & Saffer, L. Regulation of F-actin stability in dendritic spines by glutamate receptors and calcineurin. *J. Neurosci.* **18**, 9835–9844 (1998).
15. Furuyashiki, T., Arakawa, Y., Takemoto-Kimura, S., Bito, H. & Narumiya, S. Multiple spatiotemporal modes of actin reorganization by NMDA receptors and voltage-gated Ca^{2+} channels. *Proc. Natl. Acad. Sci. USA* **99**, 14458–14463 (2002).
16. Furukawa, K. *et al.* The actin-severing protein gelsolin modulates calcium channel and NMDA receptor activities and vulnerability to excitotoxicity in hippocampal neurons. *J. Neurosci.* **17**, 8178–8186 (1997).
17. Star, E.N., Kwiatkowski, D.J. & Murthy, V.N. Rapid turnover of actin in dendritic spines and its regulation by activity. *Nat. Neurosci.* **5**, 239–246 (2002).
18. Wang, Y.L. & Taylor, D.L. Probing the dynamic equilibrium of actin polymerization by fluorescence energy transfer. *Cell* **27**, 429–436 (1981).
19. Taylor, D.L., Reidler, J., Spudich, J.A. & Stryer, L. Detection of actin assembly by fluorescence energy transfer. *J. Cell Biol.* **89**, 362–367 (1981).
20. Miyawaki, A. *et al.* Fluorescent indicators for Ca^{2+} based on green fluorescent proteins and calmodulin. *Nature* **388**, 882–887 (1997).
21. Giepmans, B.N., Adams, S.R., Ellisman, M.H. & Tsien, R.Y. The fluorescent toolbox for assessing protein location and function. *Science* **312**, 217–224 (2006).
22. Stoppini, L., Buchs, P.A. & Muller, D. A simple method for organotypic cultures of nervous tissue. *J. Neurosci. Methods* **37**, 173–182 (1991).
23. Shi, S.H. *et al.* Rapid spine delivery and redistribution of AMPA receptors after synaptic NMDA receptor activation. *Science* **284**, 1811–1816 (1999).
24. Lo, D.C., McAllister, A.K. & Katz, L.C. Neuronal transfection in brain slices using particle-mediated gene transfer. *Neuron* **13**, 1263–1268 (1994).
25. Arnold, D., Feng, L., Kim, J. & Heintz, N. A strategy for the analysis of gene expression during neural development. *Proc. Natl. Acad. Sci. USA* **91**, 9970–9974 (1994).
26. Hayashi, Y. *et al.* Driving AMPA receptors into synapses by LTP and CaMKII: requirement for GluR1 and PDZ domain interaction. *Science* **287**, 2262–2267 (2000).
27. Miyawaki, A. Innovations in the imaging of brain functions using fluorescent proteins. *Neuron* **48**, 189–199 (2005).
28. Campbell, R.E. *et al.* A monomeric red fluorescent protein. *Proc. Natl. Acad. Sci. USA* **99**, 7877–7882 (2002).
29. Shaner, N.C. *et al.* Improved monomeric red, orange and yellow fluorescent proteins derived from *Discosoma* sp. red fluorescent protein. *Nat. Biotechnol.* **22**, 1567–1572 (2004).
30. Vanderklish, P.W. *et al.* Marking synaptic activity in dendritic spines with a calpain substrate exhibiting fluorescence resonance energy transfer. *Proc. Natl. Acad. Sci. USA* **97**, 2253–2258 (2000).
31. Takao, K. *et al.* Visualization of synaptic Ca^{2+}/calmodulin-dependent protein kinase II activity in living neurons. *J. Neurosci.* **25**, 3107–3112 (2005).
32. Denk, W., Strickler, J.H. & Webb, W.W. Two-photon laser scanning fluorescence microscopy. *Science* **248**, 73–76 (1990).
33. Denk, W. & Svoboda, K. Photon upmanship: why multiphoton imaging is more than a gimmick. *Neuron* **18**, 351–357 (1997).
34. Mainen, Z.F. *et al.* Two-photon imaging in living brain slices. *Methods* **18**, 231–239 181 (1999).
35. Nagai, T. *et al.* A variant of yellow fluorescent protein with fast and efficient maturation for cell-biological applications. *Nat. Biotechnol.* **20**, 87–90 (2002).
36. Matsuzaki, M. *et al.* Dendritic spine geometry is critical for AMPA receptor expression in hippocampal CA1 pyramidal neurons. *Nat. Neurosci.* **4**, 1086–1092 (2001).